ADVANCED
MATERIALS
TECHNOLOGIES

One-Step Selective Adhesive Transfer Printing for Scalable Fabrication of Stretchable Electronics

Peng Peng, Kang Wu, Liangxiong Lv, Chuan Fei Guo, and Zhigang Wu*

Transferring patterned thin foil structures onto an elastic substrate is one important process for realizing heterogeneous integration and high-performance stretchable electronics. Usually, specific equipment and long learning curve are necessary for transferring fragile micro/nanostructures. In this work, a one-step selective transfer printing technique can selectively transfer fine metal structure from a donor substrate to a sticky polydimethylsiloxane receiver by tuning its adhesion force and hence corresponded energy release rate (*G*). The method greatly simplifies the transferring process compared with traditional ones. The selective transferring lies in the fact that a wider line requires a higher energy release rate, based on experimental and numerical analysis. With the selective adhesive transferring technique, a few simple stretchable devices and structures are fabricated, where a device does not exhibit any fatigue after stretching for 10 000 cycles under a 40% strain. Further, this method does not use any new specific equipment and is believed to be a reliable and cost-effective technique for potential mass production of stretchable electronics.

1. Introduction

Stretchable electronics have attracted a lot of attentions due to the ability to be bent, twisted, stretched, and deformed into diverse shapes.[1] These unique and novel properties will be extensively applied in electronic devices, such as electronic eyeball camera,[2] epidermal electronics,[3] monitoring and therapy device,[4] and flexible pressure sensors.[5] The integration of material/mechanical design and fabrication technique play a key role in the development of stretchable electronics.[6–9] Devices with stretchability range from 30% to 300% responds to the deformation in or out of plane[10] have been presented by introducing innovative structures such as compressive buckling,[11–14] special designed mesh.[15,16] However, the traditional stretchable electronics manufacture based on standard fabrication processes includes vacuum deposition of metal film,

photolithography, etching, and transfer printing.[17] Vacuum deposition of metal film, photolithography, and etching are used to make high-precision devices, but there are problems such as environmental pollution, complicated processes, high cost and incompatibility with roll-to-roll process, and thus may limit possible industrialization.

To fabricate stretchable electronics in a simple and quick way, a "Cut and Paste" method has been proposed.[17] A benchtop cutting machine was used to pattern the metal foil. The whole process can be completed in 10 min without any wet process. Unfortunately, the accuracy of this method is limited, typically only suitable for structures with a width greater than 200 μm and the excess parts need to be removed manually making it not a good method for industrialization. For scalable manufacture of high precision stretchable electronics, we present a laser marker patterned metal circuitry and a one-step selective transfer printing technique in this work.

Many strategies are developed for transfer printing, such as thermomechanical response of elastomeric stamp with a laser,[18] temperature response of shape memory polymers (SMP),[19,20] and controlling of energy release rate to an elastomeric stamp by controlling separation speed,[21] bending radius,[22] microstructure.[23] Transferring patterned thin-film structures onto an elastic substrate has been widely used for the fabrication of stretchable electronics. It is regarded as an important and efficient process for realizing heterogeneous integration and high-performance stretchable electronics. This method can not only broaden the range of materials including rigid inorganic and deformable organic ones,[24] but also achieve cost-effective large-scale coverage and be used to make three dimensional circuits.[17,25] Efficient transfer depends on the switching energy release rate between the donor and receiver substrate. Nevertheless, it is still tricky to control the transferring process in practical operations. Often, specific equipment and a long learning curve are required for such transfer printing techniques. Moreover, in the above strategies, the selection of the transferring material/components highly relies on the stamp and targeting material together with corresponding patterning techniques. Regarding the transfer stamp, polydimethylsiloxane (PDMS) is a widely used material due to its high performance and flexibility in the practical implementations. Previously, many ways have been investigated to modify the surface properties of PDMS such as oxide plasma treatments, ultra violet light

P. Peng, Dr. K. Wu, L. X. Lv, Prof. Z. G. Wu
State Key Laboratory of Digital Manufacturing Equipment and Technology
Huazhong University of Science and Technology
Wuhan 430074, China
E-mail: zgwu@hust.edu.cn, Zhigang.Wu@angstrom.uu.se
Prof. C. F. Guo
Department of Materials Science & Engineering
Southern University of Science & Technology
Shenzhen, Guangdong 518055, China

**ADVANCED
SCIENCE NEWS**
www.advancedsciencenews.com

**ADVANCED
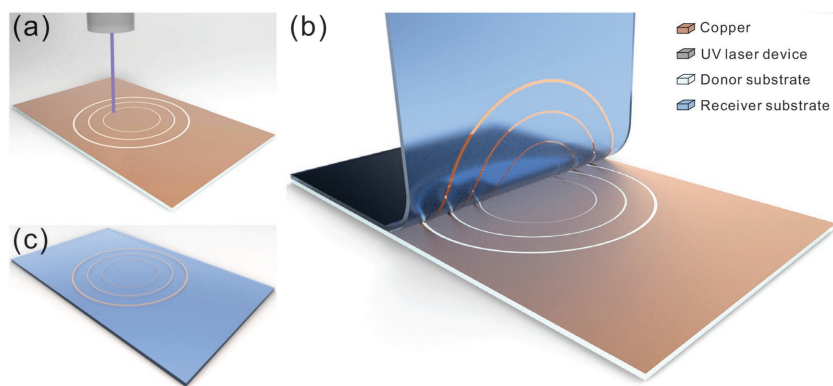MATERIALS
TECHNOLOGIES**
www.advmattechnol.de

Figure 1. Schematic illustration of the steps of selective transfer printing: a) copper foil patterning by UV laser; b) selective transfer the required copper pattern; c) copper pattern on the receiver substrate. Both of the donor and receiver are based on PDMS but their energy release rates are different.

irradiation, buffered oxide etchant NaOH etching.[24] However, these methods rely on well-trained operational staffs and specific equipment, which would be counterproductive to low-cost and high-efficiency production. Recently, we have shown a tunable adhesive PDMS-based elastomer by simply adding a tiny amount of an amine-based polymer (0-30 μL polyethylenimine, PEIE, per 10 g PDMS), which provides a simple and effective way to tune the adhesion of PDMS.[26]

By introducing a tunable adhesive PDMS as well as the receiver substrate and controlling the line width of laser ablated copper lines on the donor substrate, here we propose a one-step technique for selective transfer printing of stretchable electronics. During the transfer process, the energy release rate can be directed controlled by tuning the adhesion force of PDMS substrate. Compared with previous approaches, the whole process of stretchable devices can be simplified to only three steps: laser cutting, selective transfer printing, and encapsulation. In our demonstration, an UV laser marker was introduced to pattern high-resolution circuits on the commercially available copper foil (Figures S1 and S2 in the Supporting Information, SI). The required metal circuitry and unnecessary copper material are sundered by UV laser on the donor substrate (**Figure 1**a). Then the copper circuit is separated

directly from the unnecessary copper material by selective transfer with a tunable stamp, as shown in Figure 1b. By controlling the added amount of PEIE, curing time and curing temperature, PDMS-based substrates with different energy release rate are prepared. The designed circuits are selected from the excess metal and then transferred from the donor to the receiver substrate due to the fact that the energy release rate is difference between them by simply controlling the line width (rigidity). Meanwhile, as the receiver substrate is a PDMS-based elastomer, the designed copper pattern on the receiver substrate is ready for encapsulation directly without further process (Figure 1c). The PDMS substrate production and UV laser operation are compatible to existing automatic production line such as roll-to-roll processing, which have high potential to be adapted to an automatic and large-scale fabrication of stretchable electronics in the future.

2. Results and Discussions

2.1. Tunable Adhesive Elastomer Stamp

By controlling the added amount of PEIE, curing time and temperature, the energy release rate differences between donor substrate and receiver substrate are realized. **Figure 2**a shows the variation of energy release rate with different amount of PEIE, with tested samples cured at 90 °C. The energy release rate is measured by a self-developed instrument (Figure S3 in the Supporting Information), via referring to the standard of American Society for Testing and Materials (ASTM) D6862-2004. Generally, stronger energy release rate can be obtained by adding more PEIE, and energy release rate declines with the curing time under a fixed PEIE amount. Meanwhile, the curing process consumes longer time when more PEIE is added.[26] This modification will enhance the ability of compliance and elongation of tuned PDMS. The increased energy release rate is mainly owing
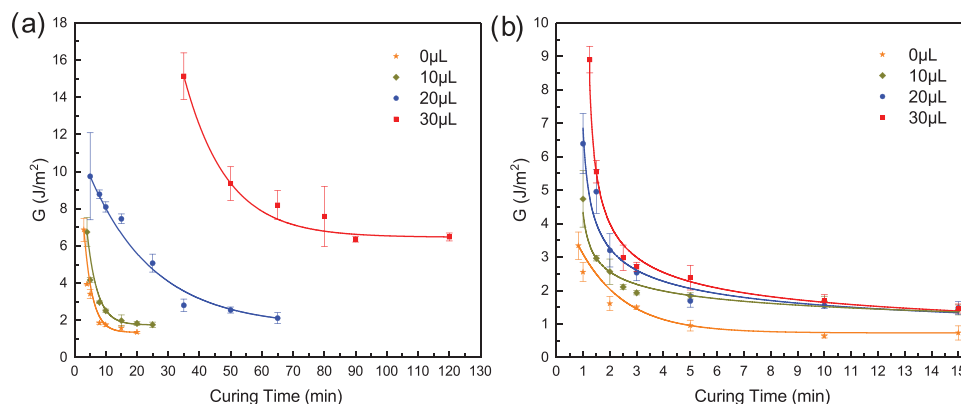

Figure 2. The energy release rates at different curing temperatures: a) energy release rate of PDMS cured at 90 °C; b) energy release rate of PDMS cured at 120 °C. Generally, stronger energy release rate can be obtained by adding more PEIE, and energy release rate declines with curing time under a fixed PEIE amount.

**ADVANCED
SCIENCE NEWS**
www.advancedsciencenews.com

**ADVANCED
MATERIALS
TECHNOLOGIES**
www.advmattechnol.de

to the extremely high compliance (low elastic modulus) and viscous surface adaptation, enhancing the corresponding van der Waals interactions. However, the continuous heat flux has a negative effect on PEIE. Figure 2b shows similar characteristics when the curing temperature increases to 120 °C, but the curing time is shortened dramatically. Since PDMS is known as a viscoelastic material and the energy release rate is a monotonically increasing function of peeling rate,[27] the peeling rate is fixed and kept low in our measurement to minimize its influence.

2.2. Selective Adhesive Transferring

To realize the separation mechanism between metal circuit and excess materials, we studied the effect of width on the transferring as shown in **Figure 3** (Videos 1.1–1.4 in the Supporting Information). The copper line of 200 µm in width can be transferred to the receiver substrate of which the energy release rate is 1.74 J m⁻² (Figure 3a). The copper lines of 200 and 400 µm width can be transferred to the receiver substrate with an energy release rate of 1.84 J m⁻² as shown in Figure 3b. The copper line of 1600 µm width or narrower can be transferred to the receiver substrate with an energy release rate of 3.41 J m⁻² as shown in Figure 3c. All copper lines can be transferred to the receiver substrate when energy release rate goes up to 6.86 J m⁻² as shown in Figure 3d. It is clear that copper lines can be selectively transferred to the receiver in a one-step process by controlling the line width and energy release rate. From the above experiments, we observed that narrower copper lines can be transferred while the wider ones cannot be transferred under the same energy release rate and receiver, as summarized in Figure 3e,f. For a single patterned copper line at a given thickness, the rigidity increases with the increasing width. When the copper line is narrower, the peeling force is strong enough to deflect the copper, and hence it can follow the deformation of the receiver. Subse-

quently, the interface between the copper line and the donor substrate cracks, and further propagates along the interface. Finally, the narrower copper line can be transferred from the donor to the receiver. By contrast, when the copper line is wider with an increased rigidity, the peeling force is not strong enough to deflect it so that it cannot follow the deformation of the receiver and stay on the donor. Hence, a selective transfer printing can be achieved at the same energy release rate.

To further understand the mechanism of selective transfer printing, we simulate the deformation of copper line with different widths in COMSOL Multiphysics 5.2 (Figure S4 in the Supporting Information), while keeping other conditions the same. The simulation results in **Figure 4**a show that the deflection varies with the width of copper under the same force. The deflection d (the deflection of the copper line at the end) decreases with the increase of width w.

Through curve fitting, the relationship of the width and deflection can be obtained as

$$d = S\,w^a = 4.249 \times 10^{-8} \times w^{-1.008} \tag{1}$$

where d is the deflection of copper line and w is the width of copper line. As stiffness is the ratio of the load to the resulting deformation. The deflection can be approximated to the deformation of copper lines, which is equal to the torque divided by the flexural rigidity

$$d = M/D = FL/D \tag{2}$$

where F is the load, L is the length of copper foil, D is the flexural rigidity, M is the torque, and F and L are constants in the simulation. From Equations (1) and (2), the relationship between w and D can be derived as

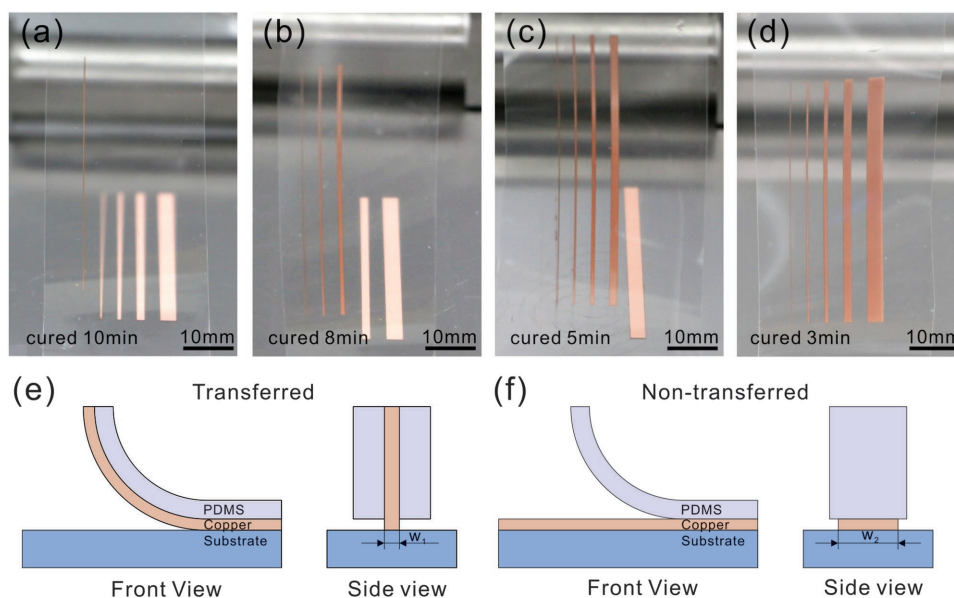$$D = \alpha w^{1.008} \tag{3}$$

Figure 3. a–d) The effect of curing time on transfer printing and e,f) corresponding schematic diagram of selective transfer printing. All receiver substrates are cured at 90 °C for a–d) 10, 8, 5, and 3 min, respectively. Each set of lines consists of copper lines at widths of 200, 400, 800, 1600, and 3200 µm.
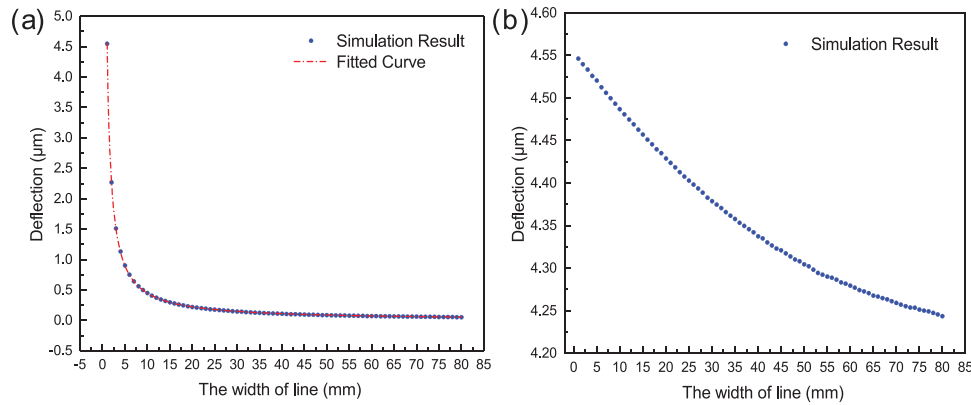
Figure 4. The deflection-simulated results of copper line: a) the force is consistent and b) the energy release rate is consistent.

Here D increases gradually with the increasing w, and α is a proportional constant. In the process of transfer printing, the comprehensive load on the copper foil ΔF is proportional to the energy release rate ΔG (which is the difference between receiver and donor) and the width w[27]

$$\Delta F = w\Delta G \tag{4}$$

According to Equation (3) and (4), the effect of width on flexural rigidity is slightly greater than that of the force. With the increase of width, the increase of flexural rigidity is greater than that of the force. Therefore, as the width increases, its deformation decreases gradually.

In Equations of (2), (3) and (4), the relationship between w and d^* can be derived in the transfer printing process

$$d^* = \Delta FL^*/D = w\Delta GL^*/kw^{1.008} = \beta w^{-0.08} \tag{5}$$

where L^* is the length of the copper foil, and β is a proportional constant. Furthermore, we simulated the deformation of copper line with different widths under the same energy release rate (Figure S4 in the Supporting Information). The result is shown in Figure 4b, where the deflection of the copper line decreases with the increasing width under the same energy release rate, which is consistent with Equation (5). The energy release rate for the delamination of the copper lines increases as width increases, which agrees well with previous study on the residual stress induced delamination of film lines from the substrate.[28]

When d^* is equal to the critical deflection d_{crit}, the corresponding energy release rate is the critical $G_{crit}^{transfer}$

$$d_{crit} = F^*L^*/D = wG_{crit}^{transfer}L^*/\alpha w^{1.008} \tag{6}$$

According to Equation (6), the relationship between $G_{crit}^{transfer}$ and w can be derived as

$$G_{crit}^{transfer} = d_{crit}\alpha w^{1.008}/wL^* = \frac{d_{crit}\alpha}{L^*}w^{0.08} = \gamma w^{0.08} \tag{7}$$

where γ is a proportional constant, and $G_{crit}^{transfer}(w)$ is a monotonically increasing function of w. Define the critical peeling force as[27]

$$F_{crit} = wG_{crit}^{transfer}(w) \tag{8}$$

When the peeling forces ΔF is larger than F_{crit}, the copper line can be transferred. The criterion for selective transfer printing is obtained by comparing ΔG and $G_{crit}^{transfer}(w)$. When $\Delta G > G_{crit}^{transfer}(w)$, the copper line can be transferred. When $\Delta G < G_{crit}^{transfer}(w)$, the copper line fails to be transferred.

The schematic of selective transfer printing is shown in **Figure 5**. Where ΔG is a horizontal line, $G_{crit}^{transfer}(w)$ is a monotonically increasing function of w. When $\Delta G_1 = G_{crit}^{transfer}(w_{crit})$ there is a critical w_{crit}. When $w_1 < w_{crit}$, $\Delta G_1 > G_{crit}^{transfer}(w_1)$ and the copper line can be transferred. When $w > w_{crit}$, $\Delta G_1 < G_{crit}^{transfer}(w_2)$ and the copper line cannot be transferred. This mechanism explains how our selective transfer printing works. When ΔG is in the range from $G_{crit}^{transfer}(w_1)$ for narrower lines to $G_{crit}^{transfer}(w_2)$ for wider ones, a selective transfer printing can be achieved by controlling the line width.

An isolated copper foil pattern with three rings (width: 100, 200, and 300 μm, from the center to the most outside) is chosen to verify afore mentioned theoretical analysis. The copper foil is
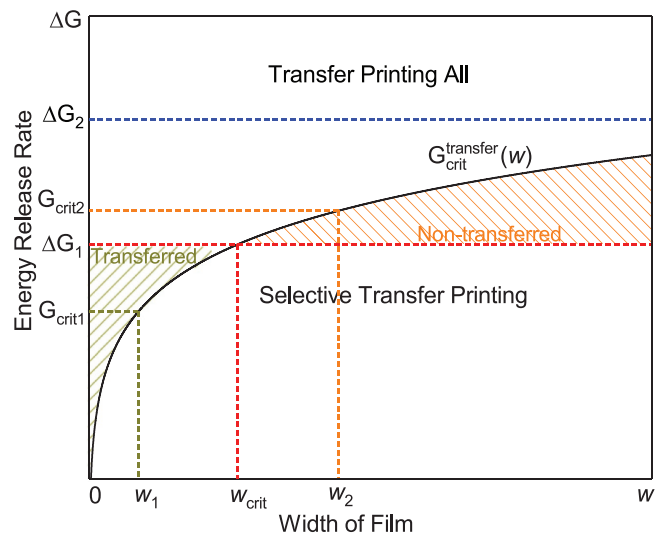

Figure 5. The schematic mechanism of selective transfer printing. When the width of the copper line $w_1 < w_{crit}$, the copper line can be transferred otherwise the copper line cannot be transferred.
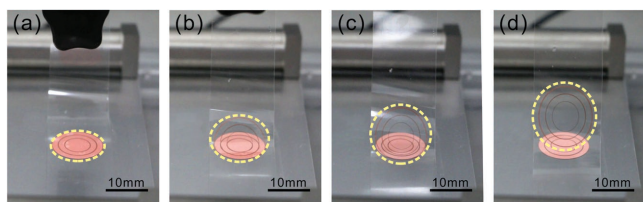
Figure 6. a–d) The serial process of selective transfer printing of rings from a laser cut copper foil.

cut into six concentric circles in which the radii are 6, 6.1, 9, 9.2, 12, 12.3 mm, respectively, by a UV laser marker. The circuit pattern widths are 100, 200, 300 μm, respectively, and the width of excess metal are 12, 6, 6 mm correspondingly. As shown in **Figure 6** (and shown in Video 2.1 in SI as well), the circuit pattern is separated from the excess metal by the receiver substrate at an energy release rate of 3.41 J m^{-2}. Further, it applies to not only copper foil, but also other materials, such as aluminum foil and polyethylene terephthalate (PET) foil in Videos 2.2 and 2.3 in SI.

2.3. Performance Test

Using the above method, stretchable connects that deforms in-plane (Figures S5 and S6 in the Supporting Information) are fabricated. To visualize the results, an LED was embedded in the PDMS substrate to demonstrate a functional circuit. As shown in **Figure 7**, the device can be stretched to 300% at a single time test without showing failure.

To study the reliability of a new fabricated stretchable copper conductor, a cyclic tensile test under a 40% strain at 0.25 Hz was conducted, as illustrated in **Figure 8**. We found that the
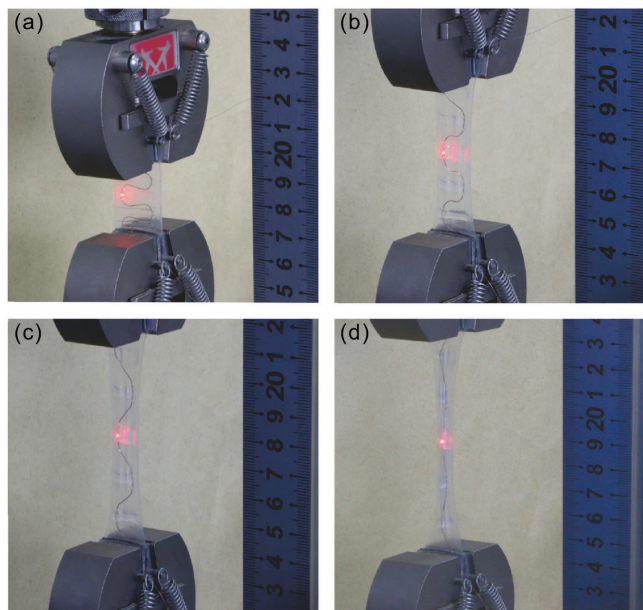

Figure 7. Test of stretchable electrode: a–d) photographs of an LED light connected to wavy copper line at strains of 0, 200%, 250%, and 300%.
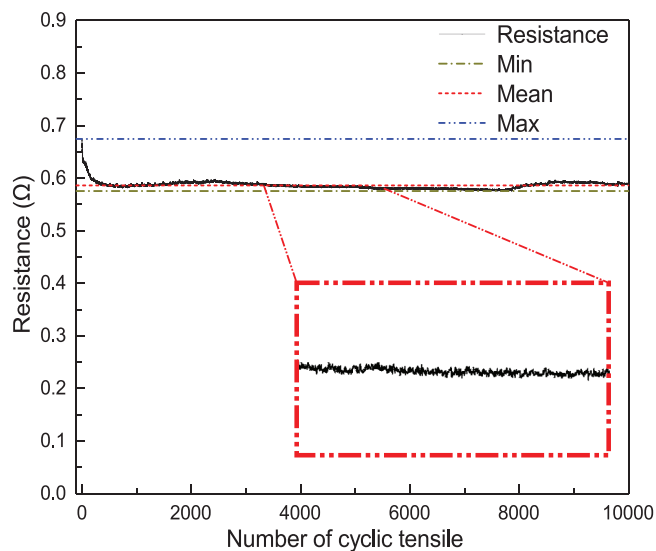

Figure 8. The cyclic stretching test. The applied strain is 40%, and each cycle lasts for 4 s.

original resistance is quite small (around 0.65 Ω) and there is a small variation during the whole 10 000 cycles of stretching and releasing. Note that there is a slight drop of resistance at the first stretch. We believe that this decrease comes from the removal of the oxide layer covered on copper lines at the contact. Overall, the resistance of connects is quite stable during cyclical stretching.

We have also fabricated stretchable connects that deform out-of-plane by selective transfer printing. We can control buckles by applying different prestrains and energy release rates of the substrate as shown in **Figure 9**. The prestrains of the PDMS substrates are 5%, 10%, and 20% in Figure 9a–c,d–f. For panels a–c, the substrate is pristine PDMS, and after releasing the prestrains only one arc is observed due to the weak energy release rate; whereas in panels d–f, the PDMS substrates are sticky, and a set of spontaneous periodic delamination are observed. Such structures have been proven to be an effective design for stretchable devices.[29] However, compared to the existing method by bonding the nanoribbons with an activated adhesive layer on a stretchable substrate, our method generates buckled shapes spontaneously, without photolithographic methods. The result indicates that our sticky PDMS can be used for making spontaneous out-of-plane buckles for stretchable electronics.

3. Summary

This work presents a one-step selective transfer printing technique that can selectively pick up desired structures while leaving unnecessary parts from the patterned metal. Further, we developed a mechanism of selective transferring mechanism by experimental investigations and numerical analysis, which indicates that transferring wider lines requires a substrate with a higher energy release rate. By tuning the energy release rate of PDMS and the width of the patterned metal, we can transfer required pattern accurately. To verify the new process, we have successfully fabricated quite a few stretchable
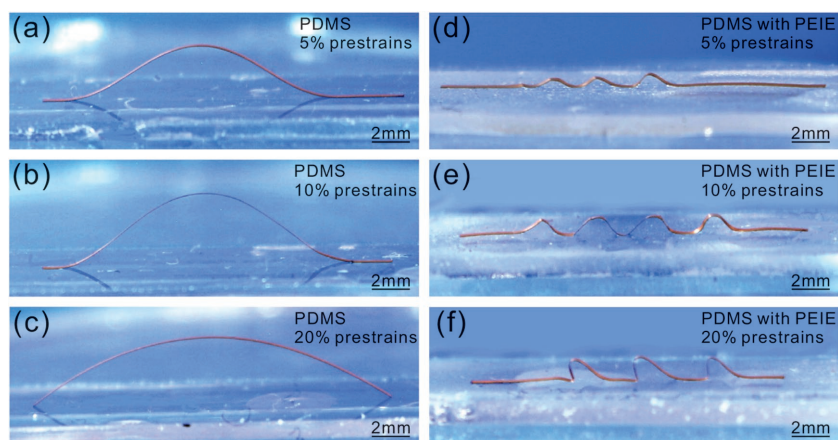
Figure 9. The waveform of released copper under different prestrains with different substrates: a–c) copper foil on normal PDMS with prestrains of 5%, 10%, and 20%, showing a single arc; d–f) copper foil on sticky PDMS with prestrains of 5%, 10%, and 20%, and periodic out-of-plane buckled structures are observed.

connects, demonstrating excellent stretchability as well as reliability. The whole process is easy to operate and maintain, and it might be further extended to roll-to-roll technique for mass production of circuits. Overall, this technology provides a new way that is potential for industrialization of stretchable electronics, which might be used for mass production.

4. Experimental Section

Patterning the Copper Foil: A UV laser marker (HGL-LSU3/5EI, Huagong Laser, Wuhan, China) was used to pattern the copper foil (EQ-bccf-9u, thinness: 9 µm, Shenzhen Kejing Star Tech, Shenzhen, China). The pulse repetition frequency was 70 kHz and the cutting speed was 95 mm s^{-1} in fabrication of stretchable electronics and the design width was more than the required width 21.3 µm.

Optical Characterization: A metallographic microscope (BA310MET-T, Motic, Xiamen, China) with a CCD camera was used to observe the quality of copper pattern. The edge topography was obtained by cutting 9 µm thick copper foil. The photograph of edge topography was obtained by upright metallurgical microscope and the edge data were processed by a self-developed codes programme.

Modification of PDMS: The PDMS (Sylgard184, Dow Corning, Michigan, America) used in this work was modified by adding a small amount (0-30 µL per 10 g PDMS) of PEIE (80% ethoxylated solution, 37 wt% in H_2O, average MW = 110 000, Sigma-Aldrich, St. Louis, USA) to the mixture of two-part liquid components (PDMS base and curing agent), which were mixed with the recommended weight ratio of 10:1 before curing. A pipette (100 µL, Eppendorf) was used to sample the PEIE solution. The PDMS base, curing agent and PEIE solution were added to a plastic cup successively and mixed together manually for 1 min with a glass rod. The so-called *n* µL modified PDMS means that there is *n* µL PEIE in every 10 g PDMS base of modified PDMS. Prior to putting into use, vacuumization (10 min) and refrigeration (about −18 °C for 15 min) were used to eliminate the air bubbles.

Preparation of the Samples for Energy Release Rate Measurement: First, a thin film of polyester (polyethylene terephthalate, PET with thinness of 50 µm) was stuck onto the surface of a smooth aluminum plate (100 mm × 150 mm × 1 mm). Second, the modified PDMS was bladed into a thin layer (thinness: 20 µm) on the PET film and consequently cured at a specific temperature and time in an oven. Third, a thin copper foil was attached uniformly to the surface of cured

modified PDMS. A roller was used to ensure the attachment tightly and evenly. Finally, by cutting the copper foil into a specific pattern via a laser marker and peeling off the extra foil, the sample was ready for energy release rate measurement.

Energy Release Rate Measurement: The energy release rate measurement setup was based on the international standard test method for 90° peeling resistance of energy release rate (Designation: ASTM D 6862-2004) and test method for peeling strength of pressure-sensitive tape (Designation: GB/T 2792-1981).

Fabrication and Characterization of the Stretchable Connects: The copper foil with surface coated by a polyimide layer was ablated into a horseshoe-shaped pattern on a cured PDMS film by the laser marker and then transferred to a substrate of Ecoflex with small PDMS rectangle stripes, for which the thickness is 100 µm, on its surface. An LED (0402, Hongguang electronic technology, Suzhou, China) was welded for visualization of the results. This device was packaged with another substrate of the same configuration. This kind of substrate with small PDMS rectangle stripes on it was made by a mask technology. A dynamic test instrument (E1000, Instron, Boston, America) together with a digital multimeter (34461A, KeySight Technologies, America) was used for stretching test.

Supporting Information

Supporting Information is available from the Wiley Online Library or from the author.

Acknowledgements

Conflict of Interest

The authors declare no conflict of interest.

Keywords

[1] J. A. Rogers, T. Someya, Y. Huang, *Science* **2010**, *327*, 5973.
[2] I. Jung, G. Shin, V. Malyarchuk, J. S. Ha, J. A. Rogers, *Appl. Phys. Lett.* **2010**, *96*, 2.
[3] D. H. Kim, N. Lu, R. Ma, Y. S. Kim, R. H. Kim, S. Wang, J. Wu, S. M. Won, H. Tao, A. Islam, K. J. Yu, T. Kim, R. Chowdhury, M. Ying, L. Z. Xu, M. Li, H. J. Chung, H. Keum, M. McCormick,

P. Liu, Y. W. Zhang, F. G. Omenetto, Y. G. Huang, T. Coleman, J. A. Rogers, *Science* **2011**, *333*, 838.

[4] H. J. Lee, T. K. Choi, Y. B. Lee, H. R. Cho, R. Ghaffari, L. Wang, H. J. Choi, T. D. Chung, N. S. Lu, T. Hyeon, S. H. Choi, D. H. Kim, *Nat. Nanotechnol.* **2016**, *11*, 6.

[5] S. C. B. Mannsfeld, B. C. K. Tee, R. M. Stoltenberg, C. V. H. H. Chen, S. Barman, B. V. O. Muir, A. N. Sokolov, C. Reese, Z. N. Bao, *Nat. Mater.* **2010**, *9*, 10.

[6] D. H. Kim, J. Xiao, J. Song, Y. Huang, J. A. Rogers, *Adv. Mater.* **2010**, *22*, 19.

[7] M. L. Hammock, A. Chortos, B. C. K. Tee, J. B. H. Tok, Z. Bao, *Adv. Mater.* **2013**, *25*, 42.

[8] S. Choi, H. Lee, R. Ghaffari, T. Hyeon, D. H. Kim, *Adv. Mater.* **2016**, *28*, 22.

[9] T. Q. Trung, N. E. Lee, *Adv. Mater.* **2017**, *29*, 3.

[10] Y. Su, X. Ping, K. J. Yu, J. W. Lee, J. A. Fan, B. Wang, M. Li, R. Li, D. V. Harburg, Y. Huang, C. Yu, S. Mao, J. Shim, Q. Yang, P. Y. Lee, A. Armonas, K. J. Choi, Y. Yang, U. Paik, T. Chang, T. J. Dawidczyk, Y. Huang, S. Wang, J. A. Rogers, *Adv. Mater.* **2017**, *29*, 1604989.

[11] D. Y. Khang, H. Q. Jiang, Y. Huang, J. A. Rogers, *Science* **2006**, *311*, 5758.

[12] D. H. Kim, J. Song, W. M. Choi, H. S. Kim, R. H. Kim, Z. Liu, Y. Y. Huang, K. C. Hwang, Y. Zhang, J. A. Rogers, *Proc. Natl. Acad. Sci. USA* **2008**, *105*, 48.

[13] D. H. Kim, Z. Liu, Y. S. Kim, J. Wu, J. Song, H. S. Kim, Y. Huang, K. Hwang, Y. Zhang, J. A. Rogers, *Small* **2009**, *5*, 24.

[14] S. Xu, Z. Yan, K. I. Jang, W. Huang, H. Fu, J. Kim, Z. Wei, M. Flavin, J. McCracken, R. Wang, A. Baddea, Y. Liu, D. Xiao, G. Zhou, J. Lee, H. U. Chung, H. Cheng, W. Ren, A. Banks, X. li, U. Paik, R. G. Nuzzo, Y. Huang, Y. Zhang, J. A. Rogers, *Science* **2015**, *347*, 154.

[15] K. I. Jang, H. U. Chung, S. Xu, C. H. Lee, H. Luan, J. Jeong, H. Cheng, G. T. Kim, S. Y. Han, J. W. Lee, J. Kim, M. Cho, F. Miao, Y. Yang, H. N. Jung, M. Flavin, H. Liu, G. W. Kong, K. J. Yun, S. Rhee, J Chung, B. Kim, J. W. Kwak, M. H. Yun, J. Y. Kim,

Y. M. Song, U. Paik, Y. Zhang, Y. Huang, J. A. Rogers, *Nat. Commun.* **2015**, *6*, 6566.

[16] S. Xu, Y. H. Zhang, J. Cho, J. Lee, X. Huang, L. Jia, J. A. Fan, Y. W. Su, J. Su, H. G. Zhang, H. Y. Cheng, B. W. Lu, C. J. Yu, C. Chuang, T. I. Kim, T. Song, K. Shigeta, S. Kang, C. Dagdeviren, I. Petrov, P. V. Braun, Y. Huang, U. Paik, J. A. Rogers, *Nat. Commun.* **2013**, *4*, 1543.

[17] S. Yang, Y. Chen, L. Nicolini, P. Pasupathy, J. Sacks, B. Su, R. Yang, D. Sanchez, Y. Chang, P. Wang, D. Schnyer, D. Neikirk, N. S. Lu, *Adv. Mater.* **2015**, *27*, 41.

[18] R. Saeidpourazar, R. Li, Y. Li, M. D. Sangid, C. Lu, Y. Huang, J. A. Rogers, P. M. Ferreira, *J. Microelectromech. Syst.* **2012**, *21*, 5.

[19] J. D. Eisenhaure, S. Rhee, A. M. Al-Okaily, A. Carlson, P. M. Ferreira, S. Kim, *J. Microelectromech. Syst.* **2014**, *23*, 5.

[20] Y. Xue, Y. Zhang, X. Feng, S. Kim, J. A. Rogers, Y. Huang, *J. Mech. Phys. Solids* **2015**, *77*, 27.

[21] M. A. Meitl, Z. Zhu, V. Kumar, K. J. Lee, X. Feng, Y. Huang, I. Adesida, R. G. Nuzzo, J. A. Rogers, *Nat. Mater.* **2006**, *5*, 1.

[22] S. Cho, N. Kim, K. Song, J. Lee, *Langmuir* **2016**, *32*, 31.

[23] S. Kim, J. Wu, A. Carlson, S. H. Jin, A. Kovalsky, P. Glass, Z. Liu, N. Ahmed, S. L. Elgan, W. Chen, P. M. Ferreira, M. S , Y. Huang, J. A. Rogers, *Proc. Natl. Acad. Sci. USA* **2010**, *107*, 40.

[24] A. Carlson, S. Wang, P. Elvikis, P. M. Ferreira, Y. Huang, J. A. Rogers, *Adv. Funct. Mater.* **2012**, *22*, 21.

[25] A. Carlson, A. M. Bowen, Y. Huang, R. G. Nuzzo, J. A. Rogers, *Adv. Mater* **2012**, *24*, 39.

[26] S. H. Jeong, S Zhang, K. Hjort, J. Hilborn, Z. G. Wu, *Adv. Mater.* **2016**, *28*, 28.

[27] X. Feng, M. A. Meitl, A. M. Bowen, Y. Huang, R. G. Nuzzo, J. A. Rogers, *Langmuir* **2007**, *23*, 25.

[28] H. H. Yu, J. W. Hutchinson. *Thin Solid Films* **2003**, *423*, 1.

[29] Y. Sun, W. M. Choi, H. Q. Jiang, Y. G. Huang, J. A. Rogers. *Nat. Nanotechnol.* **2006**, *1*, 3.

1700264 (7 of 7)